Higher-order contributions to fine structure in high-L Rydberg states of Si^{2+}

E. L. Snow
Department of Physics, SUNY Fredonia, Fredonia, New York 14063, USA

S. R. Lundeen
Department of Physics, Colorado State University, Fort Collins, Colorado 80523, USA

(Received 16 February 2007; published 27 June 2007)

Measured fine-structure patterns of high-L Rydberg states have often been used to extract measurements of both the dipole and the quadrupole polarizability of their positive ion cores. Dipole polarizabilities deduced in this way are apparently quite accurate, judging by comparison with calculated values, but the accuracy of quadrupole polarizabilities is questionable. The polarizabilities of Na-like silicon are a good example. Recent fine-structure measurements seem to imply a quadrupole polarizability, in clear disagreement with calculations. This apparent discrepancy is due to misinterpretation of the experimental data, neglecting the effects of higher-order terms in the polarization potential that significantly alter the slope of the traditional polarization plots. When these terms are calculated, and their magnitude estimated, the discrepancy is eliminated. The implications of the higher-order terms for analysis of high-L fine-structure patterns are discussed.

DOI: 10.1103/PhysRevA.75.062512 PACS number(s): 32.10.Dk, 32.10.Fn, 32.30.Bv

INTRODUCTION

The deviation from pure hydrogenic values of the binding energies of nonpenetrating high-L Rydberg states with S-state cores can be expressed as the expectation value of an effective potential.

$$V_{eff}(r) = -\frac{C_4}{r^4} - \frac{C_6}{r^6} - \frac{C_7}{r^7} - C_{8L}\frac{L(L+1)}{r^8} - \frac{C_8}{r^8} + \cdots, \quad (1)$$

where each coefficient C_i is a property of the free ion core. Since the expectation value of r^{-s} decreases rapidly with increasing s for high-L states, the expectation value of V_{eff} can be rapidly convergent, giving a precise account of the Rydberg fine structure for a very wide range of Rydberg states. The most complete theoretical treatment of this approach occurs in the helium atom, where Drachman has proved the connection between the effective potential and the Rydberg energies and calculated each C_i coefficient analytically for the case of a He^+ core ion [1]. In the more general case, a nonpenetrating high-L Rydberg electron bound to a multielectron S-state ion, the connection remains valid since its derivation requires only a zeroth-order hydrogenic Rydberg wave function. However, the coefficients become functions of the wave functions and energies of the core ion. In particular, it has long been known that

$$C_4 = \frac{\alpha_d}{2}, \quad C_6 = \frac{1}{2}(\alpha_Q - 6\beta_d), \quad (2)$$

where

$$\alpha_d = \frac{2}{3}\sum_{n_c}\frac{|\langle gS\|\vec{D}\|n_cP\rangle|^2}{E(n_cP)},$$

$$\alpha_Q = \frac{2}{5}\sum_{n_c}\frac{|\langle gS\|\overleftrightarrow{Q}\|n_cD\rangle|^2}{E(n_cD)},$$

$$\beta_d = \frac{1}{3}\sum_{n_c}\frac{|\langle gS\|\vec{D}\|n_cP\rangle|^2}{E(n_cP)^2}, \quad (3)$$

and $\vec{D}$ and $\overleftrightarrow{Q}$ represent the dipole and quadrupole moment operators acting on the $(N-1)$-electron core ion,

$$\vec{D} = \sum_{i=1}^{N-1} r_i C^{[1]}(\Omega_i), \quad \overleftrightarrow{Q} = \sum_{i=1}^{N-1} r_i^2 C^{[2]}(\Omega_i). \quad (4)$$

where $C(\Omega)$ is a convenient notation for the spherical harmonics, and $E(n_CP)$ and $E(n_CD)$ represent the excitation energies of the excited P and D states of the core ion. The parameters α_d and α_Q are the dipole and quadrupole polarizabilities of the core ion, and β_d is the first "nonadiabatic" correction to the dipole polarizability [2].

Since there are only a few parameters in Eq. (1), the nonpenetrating Rydberg states are arranged in very systematic patterns. One way these patterns can be illustrated is to scale the fine-structure intervals between different Rydberg levels of the same principal quantum number with the well-known hydrogenic expectation values of $\langle r^{-s}\rangle_{nL}$ [3] to form a "polarization plot"

$$\frac{\Delta E}{\Delta\langle r^{-4}\rangle} \quad \text{vs} \quad \left(\frac{\Delta\langle r^{-6}\rangle}{\Delta\langle r^{-4}\rangle}\right). \quad (5)$$

This is similar to the procedure suggested by Edlen [4], which is often used to determine the ionization limit of a Rydberg series of fixed L, but now applied to a set of energy intervals within the same n. In many cases, this results in an approximately linear plot. Some slight curvature can be accounted for by fitting the data to the expression

$$\frac{\Delta E}{\Delta\langle r^{-4}\rangle} = B_4 + B_6\left(\frac{\Delta\langle r^{-6}\rangle}{\Delta\langle r^{-4}\rangle}\right) + B_8\left(\frac{\Delta\langle r^{-8}\rangle}{\Delta\langle r^{-4}\rangle}\right). \quad (6)$$

The fitted intercept B_4 is identified as C_4, giving an experimental estimate of α_d. The fitted slope B_6 is often interpreted

as C_6 and used to estimate $\alpha_Q - 6\beta_d$. This interpretation rests on the assumption that the contributions of higher-order terms proportional to C_7 and C_{8L} will not affect the initial slope of the scaled plot, but only introduce curvature.

In recent years, as the precision of theoretical calculations of these properties has improved, and as more precise experimental measurements have also appeared, it has become possible to test the accuracy of this interpretation of Rydberg fine-structure measurements. The case of Si^{2+} presents a good example. A recent experimental study of $n=29$ Rydberg levels with $8 \leq L \leq 14$ determined [5]

$$B_4 = 3.702(6) \text{ a.u.}, \quad B_6 = -14.6(1.6) \text{ a.u.}$$

If these fitted coefficients were identified with C_4 and C_6, they would imply

$$\alpha_d = 7.404(12), \quad \beta_d \cong 11.3, \quad \alpha_Q \cong 39,$$

where the approximate value of β_d is obtained from Eq. (3) under the assumption that the lowest excited P state at 0.3262 a.u. is the dominant contribution to both α_d and β_d.

In this case, the core ion is Na-like silicon. Atomic theory is quite accurate for such a system with one electron outside a closed shell. Theoretical calculations of the matrix elements involved in determining the core ion properties were carried out using the relativistic all-order method [6]. The calculated values of the core ion properties α_d, α_Q, and β_d are [7]

$$\alpha_d = 7.418(9), \quad \beta_d = 11.0, \quad \alpha_Q = 11.2,$$

resulting in the predicted coefficients

$$C_4 = 3.709(5) \text{ a.u.}, \quad C_6 = -27.4 \text{ a.u.}$$

The agreement between B_4 and C_4 is excellent, leading to excellent agreement between experimental and theoretical estimates of α_d. However, the agreement between B_6 and C_6 is very poor, leading to almost a factor of 4 discrepancy between the inferred value of α_Q and theory. This dramatic disagreement, far outside the uncertainties of both experiment and theory, motivated this study. Though this case is more clearly defined, it is reminiscent of other disagreements noted in Rydberg systems, for either the slope B_6 [8] or the quadrupole polarizability derived from it [9].

In this case, for the $n=29$ high-L Rydberg levels of Si^{2+}, the apparent discrepancy can be traced to the incorrect assumption that the contributions of higher-order terms in Eq. (1) will not affect the initial slope of the polarization plot, B_6. It should be clear that this is a questionable assumption by examination of Fig. 1, which shows the contributions of terms proportional to C_6, C_7, and C_{8L} to a plot such as Eq. (5), for the specific fine-structure intervals reported in the silicon study [5], assuming a unit coefficient for each term. For this choice of intervals, while the C_6 term is the most important contributor to the slope, both C_7 and C_{8L} appear to contribute significantly. To evaluate the contributions of the C_7 and C_{8L} terms to the fitted slope of the experimental data, these two terms were fitted to the same function in Eq. (6), using the same relative weights as in the experimental report. From these fits, it was determined that

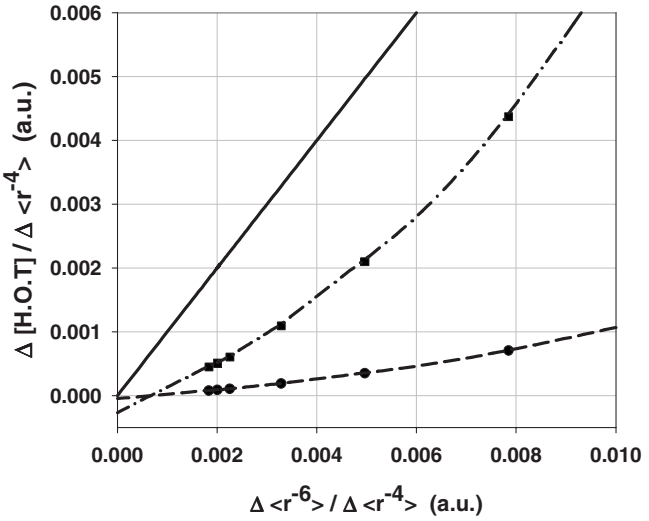

FIG. 1. Potential contributions of the higher-order terms (HOT) in Eq. (1) proportional to $\langle r^{-7} \rangle$ and $L(L+1)\langle r^{-8} \rangle$ to a normalized plot like Eq. (5) in the text. The plotted points correspond to the intervals measured in the Si^{2+} study of [5]. The x axis, $\Delta\langle r^{-6} \rangle / \Delta\langle r^{-4} \rangle$, is a decreasing function of L, so the plotted points increase in L from right to left. The solid line is a plot of this same function, for comparison. The circles represent the function $\Delta\langle r^{-7} \rangle / \Delta\langle r^{-4} \rangle$, and the squares represent the function $L(L+1) \times \langle r^{-8} \rangle / \Delta\langle r^{-4} \rangle$. Each of these terms can contribute to the slope B_6 of a plot of normalized energy differences if their coefficients are sufficiently large. The dashed and dash-dotted curves represent fits of these functions to Eq. (6) of the text, showing that each is well represented by this functional form, and determining the contribution of each to the fitted value of B_6.

$$B_6 = C_6 + 0.056C_7 + 0.302C_{8L}. \tag{7}$$

Depending on the size of the coefficients C_7 and C_{8L}, the fitted experimental slope may differ considerably from the prediction based solely on C_6. In order to assess the significance of this correction, it is necessary to calculate those coefficients.

THEORY

We assume a nonrelativistic atom, with a single distinguishable nonpenetrating Rydberg electron outside a core ion with an S-state ground state. For simplicity all spins are neglected. The eigenvalues can be developed in a perturbation series, starting from the zeroth-order states which are products of the free ion ground state, denoted by g, and a single hydrogenic Rydberg electron.

$$\Psi^{[0]} = \Psi_{core}(g)\Psi_{nLm}(\vec{r}_N). \tag{8}$$

The perturbation V contains all the Coulomb interactions excluded from the zeroth-order Hamiltonian [9]:

$$V = \sum_{i=1}^{N-1} \sum_{\kappa=1}^{\infty} \frac{r_i^\kappa}{r_N^{\kappa+1}} C^{[\kappa]}(\Omega_i) C^{[\kappa]}(\Omega_N). \tag{9}$$

The energy of the Rydberg level is given in perturbation theory by

TABLE I. Matrix elements [6,7] and excitation energies [10] used to estimate the values of coefficients δ and γ, using Eqs. (13) of the text.

Transition	Dipole	Energy (a.u.)	Transition	Quadrupole	Energy (a.u)
$3S$-$3P$	1.87	0.326	$3S$-$3D$	4.58	0.731
$3P$-$3D$	2.99		$3P$-$3P$	−5.317	

$$E(g,nL) = E^{[0]} + E^{[2]} + E^{[3]} + \cdots, \tag{10}$$

where the first-order perturbation energy is zero for an S-state core and a nonpenetrating Rydberg electron. The energy denominators that occur in $E^{[2]}$ and $E^{[3]}$ are sums of the energy differences in the two parts of the zeroth-order energy, and can be formally expanded using the "adiabatic expansion"

$$\frac{1}{\Delta E_C + \Delta E_R} = \frac{1}{\Delta E_c} - \frac{\Delta E_R}{(\Delta E_C)^2} + \frac{(\Delta E_R)^2}{(\Delta E_C)^3} - \cdots, \tag{11}$$

where ΔE_C and ΔE_R are the changes in energy of the ion core and Rydberg electron, respectively. The first term in Eq. (11) leads to the adiabatic terms, and subsequent terms lead to a sequence of nonadiabatic corrections. Using the specific properties of hydrogenic wave functions and the multipole expansion of V, both $E^{[2]}$ and $E^{[3]}$ can be expressed as the expectation value of Eq. (1) over the Rydberg radial wave function with other terms involving higher inverse powers neglected. Transforming Eq. (10) into this form is most easily accomplished using the identities of Appendix A.

The leading term in $E^{[2]}$ is the adiabatic $(\kappa=\kappa'=1)$ term, which leads to the first term in Eq. (1), proportional to C_4. The similar term with $(\kappa=\kappa'=2)$ leads to the portion of C_6 proportional to α_Q, while the part proportional to β_d comes from the first nonadiabatic correction to the $(\kappa=\kappa'=1)$ term. The C_7 term in Eq. (1) comes partly from the lowest-multipole, adiabatic contribution to $E^{[3]}$, and partly from the second nonadiabatic correction to the $(\kappa=\kappa'=1)$ term in $E^{[2]}$, which is also responsible for the term proportional to C_{8L}. The coefficient C_8 would contain contributions from several terms, and it is not calculated here. We find

$$C_7 = -\left(\frac{\delta}{2} + \frac{8Q}{5}\gamma\right), \quad C_{8L} = \frac{18}{5}\gamma, \tag{12}$$

where

$$\gamma \cong \frac{1}{6}\sum_{n_C} \frac{|\langle g\|\vec{D}\|n_C P\rangle|^2}{E(n_C P)^3}, \tag{13a}$$

$$\delta \cong \frac{4\sqrt{2}}{15}\sum_{n_C,n_C'} \frac{\langle g\|\vec{D}\|n_C P\rangle\langle n_C P\|\vec{D}\|n_C' D\rangle\langle n_C' D\|\vec{\vec{Q}}\|g\rangle}{E(n_C P)E(n_C' D)} + \frac{2\sqrt{30}}{45}\sum_{n_C,n_C'} \frac{\langle g\|\vec{D}\|n_C P\rangle\langle n_C P\|\vec{\vec{Q}}\|n_C' P\rangle\langle n_C' P\|\vec{D}\|g\rangle}{E(n_C P)E(n_C' P)}. \tag{13b}$$

Our notation is parallel to that established by Drachman in the case of helium [1], and aside from expressing the coefficients α_d, α_Q, β_d, δ, and γ in terms of core matrix elements and energy differences, our result differs only by generalizing to the case of a nonhydrogenic core ion with charge Q not necessarily equal to 1.

For positive ions in which the spin-orbit coupling in intermediate P and D states is not negligible, the results of Eqs. (3) and (13) can be generalized to include the spin-orbit energies. The results of this calculation are reported in Appendix B.

APPLICATION

For a quantitative estimate of the effects of the higher-order terms on the fits of the $n=29$, Si^{2+} data, the coefficients δ and γ must be evaluated. For the case of the Na-like Si ion, the contributions of the lowest excited states of P and D symmetry should dominate. Therefore, truncating Eqs. (13) and including only $n_C=n_C'=3$ should produce a good approximate value for δ and γ. Table I lists calculated matrix elements [6,7] and the excitation energies [10] necessary to find δ and γ in this approximation. The results are

$$\delta \cong 83.1 \text{ a.u.}, \quad \gamma \cong 16.8 \text{ a.u.}$$

Using these approximate values of δ and γ, the coefficients C_7 and C_{8L} can be estimated and their effect on the fitted slope B_6 evaluated:

$$C_7 \cong -\left(\frac{83.1}{2} + \frac{24}{5}\times 16.8\right) = -122.2 \text{ a.u.},$$

$$C_{8L} \cong \frac{36\times(16.8)}{10} = 60.5 \text{ a.u.}$$

This leads to a theoretical estimate of the fitted slope B_6 using Eq. (7):

$$B_6 \cong -27.4 - 6.8 + 18.3 = -15.9 \text{ a.u.}$$

This prediction is completely consistent with the experimental result,

$$B_6^{\text{expt}} = -14.5 \pm (1.6) \text{ a.u.}$$

Thus, the effects of the higher-order terms in the polarization potential are seen to completely resolve the apparent contradiction between theoretical predictions and experimental results. Of course, a more complete evaluation of δ and γ, avoiding the truncation of Eqs. (13) used here, would make better use of the experimental result.

It should be noted that the influence of the higher-order terms proportional to C_7 and C_{8L} on the fitted intercept B_4,

while very slight, is not entirely negligible. In the case of $n=29$ Si^{2+}, it is found that

$$B_4 = C_4 - 0.000\,053C_7 - 0.000\,290C_{8L}. \quad (14)$$

Using the estimates of C_7 and C_{8L} listed above, and the fitted value of B_4 [5], this modifies the inferred value of α_d by about 0.3%,

$$C_4 = 3.702(6) - 0.006 + 0.017 = 3.713(6),$$

$$\alpha_d = 7.426(12)\ \text{a.u.}$$

This result is in slightly better agreement with theoretical calculations than the result based on analysis without consideration of the higher-order terms [5].

The coefficients δ and γ can also be evaluated with the more complete expressions given in Appendix B and the additional matrix elements tabulated there, without significantly changing the results.

DISCUSSION

The central conclusion to be drawn from this study is that, even when a fine-structure data pattern is accurately parametrized by a fit to Eq. (6), it may not be justified to identify the fitted parameters B_4 and B_6 with the coefficients of the effective potential C_4 and C_6. If the contributions of higher-order terms in the effective potential proportional to $\langle r^{-7}\rangle$ and $L(L+1)\langle r^{-8}\rangle$ are significant, they can substantially alter the interpretation of the traditional polarization plots. This is especially true for the coefficient B_6, which in the case of Si^{2+}, $n=29$ differed by a factor of 2 from C_6, but it is also true to a lesser extent of the parameter B_4. As a consequence, it will be important for future works to at least estimate the size of these higher-order terms before drawing any conclusions from the fitted parameters. One particular case where published conclusions will need to be revised is the study of barium Rydberg levels [9] where a value of α_Q was inferred from the measured fine-structure pattern without consideration of the higher-order terms.

This is not to say that these terms are always important; in many cases they may make negligible contributions and not alter the simplest interpretation of the experimental data pattern. One way to quickly estimate the probable size of these terms is to note that the coefficient γ is likely to be the largest contributor, as it is here. If the dipole polarizability is dominated by the lowest excited P state, as it is in Si^{3+}, then γ is related to α_d by the approximation

$$\gamma \cong \frac{\alpha_d}{4E(P)^2}. \quad (15)$$

Given an estimate of α_d, from either theory or experiment, this provides an estimate of C_{8L} and, through Eqs. (7) and (14), an estimate of the probable contribution to the fitted coefficients B_4 and B_6. These estimates, of course, depend on the specific intervals measured and included in the fit. Comparison with the observed values of B_4 and B_6 then indicates whether the contribution of the higher-order terms is likely to be significant. Table II compares two cases where recent measurements exist: Si^{2+} [5] and Si^{+} [11]. It shows the value of γ that would be estimated in this approximation, the coefficient of C_{8L} in the determination of B_4 and B_6 determined from a fit similar to Eq. (6), and the probable contribution of C_{8L} to B_4 and B_6 for both cases. In this approximation, the significance of the higher-order terms appears to be negligible at the level of precision of the Si^{+} study, but quite significant in the Si^{2+} study, as the discussion above confirms. Certainly, it would be preferable to have more precise theoretical estimates of the coefficients δ and γ in any particular case.

TABLE II. Rough estimate of the contribution of C_{8L} to the fitted parameters B_4 and B_6 for two cases where recent measurements exist: Si^{2+}, $n=29$ [5] and Si^{+}, $n=19$ [11]. This estimate is obtained from the value of α_d inferred from experimental data and the excitation energy of the lowest P state of the positive ion core, using Eq. (15) of the text. The coefficients ε_{8L}^4 and ε_{8L}^6 are derived from fits of the function $\Delta[L(L+1)\langle r^{-8}\rangle]/\Delta\langle r^{-4}\rangle$ for the specific intervals and relative weights reported in the experimental studies, as in Eqs. (7) and (14) of the text. The estimated contributions to the fitted coefficients B_4 and B_6 are shown along with, for comparison, the values reported in the experiments. The effects of the higher-order term proportional to C_{8L} appear to be much less significant in the Si^{+} study than in the Si^{2+} study.

Property	Si^{2+}, $n=29$	Si^{+}, $n=19$
α_d (a.u.)	7.43	11.66
$E(P)$ (a.u.)	0.3262	0.8288
C_{8L} (estimate)	63	15
ε_{8L}^4	-2.9×10^{-4}	-1.3×10^{-5}
ε_{8L}^6	0.302	0.08
ΔB_4	0.018	0.0002
B_4^{obs}	3.702(6)	5.833(2)
ΔB_6	19	1.2
B_6^{obs}	−14.5(1.6)	−27(3)

Another conclusion that can be drawn from this study is that, even if the higher-order terms in V_{eff} proportional to C_7 and C_{8L} are significant in the fine-structure pattern, the data pattern will still be accurately parametrized by Eq. (6). This can be shown directly by fitting the higher-order contributions separately to Eq. (6) as was done above to obtain Eq. (7) and is illustrated in Fig. 1. Although these fits are not exact, they are precise enough that it seems impractical to attempt to extract additional information from the data pattern beyond the fitted coefficients B_4, B_6, and B_8. The single coefficient B_6 is likely to be the only information available from the fine-structure data pattern relating to the effective potential coefficients C_6, C_7, and C_{8L}. On the one hand, this complicates the job of extracting unambiguous information about the ion core, since prediction of B_6 requires calculation of four independent core properties α_Q, β_d, δ, and γ. On the other hand, it also widens the range of core matrix elements that can be checked by a measurement of B_6, including some dipole and quadrupole matrix elements that are not easily checked by other measurements.

The good agreement found here between theoretical and experimental values of B_6 contrasts with the situation in

TABLE III. Matrix elements between *nLJ* states [6,7] and excitation energies [10].

Transition	Dipole	Energy (a.u.)	Transition	Quadrupole	Energy (a.u)
$3S_{1/2}$-$3P1/2$	1.530	0.324810	$3S_{1/2}$-$3D3/2$	−4.105	0.730725
$3S_{1/2}$-$3P_{3/2}$	2.165	0.326911	$3S_{1/2}$-$3D_{5/2}$	5.028	0.730720
$3P_{1/2}$-$3D_{3/2}$	2.436		$3P_{1/2}$-$3P_{3/2}$	4.341	
$3P_{3/2}$-$3D_{3/2}$	1.091		$3P_{3/2}$-$3P_{3/2}$	−4.341	

lower-L Rydberg states of Si^{2+}, where polarization plots based on 3*sng*, 3*snh*, and 3*sni* Rydberg energies show dramatic variation in slopes [12]. It is well established that core penetration effects are significant in *nf* Rydberg levels and that these influence the slope of polarization plots since their contributions to the Rydberg binding energy scale with n approximately like $\langle r^{-6}\rangle$ [13,14]. The extent of core penetration contributions to Rydberg levels with $L>3$ is less well understood, though it has been suggested that these could also be responsible for the slope variations seen in 3*sng*, 3*snh*, and 3*sni* levels of Si III [12]. Calculations of penetration effects in $L>4$ levels predict effects that drop by almost two orders of magnitude with each unit increase in L [15], but these have not been confirmed by experiment. The improved understanding of the long-range interactions found here may help to clarify the extent of core penetration effects present in these lower-L Rydberg levels.

ACKNOWLEDGMENTS

This work was supported by the Chemical Sciences, Geosciences, and Biosciences Division of the Office of Basic Energy Science, Office of Science, U.S. Department of Energy. We are grateful to the theory group of Marianna Safronova for frequent assistance, and especially for providing the theoretical calculations of the matrix elements critical to this study.

APPENDIX A

Equations for reducing the first and second nonadiabatic corrections are as follows:

$$\sum_{n'} |\langle n',l'|r^{s}|n,l\rangle|^2 = \langle r^{2s}\rangle_{nl}, \tag{A1}$$

$$\sum_{n'} |\langle n',l'|r^{-s}|n,l\rangle|^2 [E(n')-E(n)] = \frac{1}{2}[s^2 - l(l+1) + l'(l'+1)]\langle r^{-2s-2}\rangle_{nl}, \tag{A2}$$

$$\begin{aligned}\sum_{n'} |\langle n',l'|r^{-s}|n,l\rangle|^2 [E(n')-E(n)]^2 = {} & \frac{1}{4}[-s(s+1) - l(l+1) + l'(l'+1)]^2 \left(\frac{1}{Q}\right)^2 \langle r^{-2s-4}\rangle_{nl} + \frac{1}{4}(2s+3)s[-s(s+1) - l(l+1) \\ & + l'(l'+1)]\left(\frac{1}{Q}\right)^2 \langle r^{-2s-4}\rangle_{nl} + (s+1)(2s+3)s^2\left(\frac{1}{Q}\right)^2 \langle r^{-2s-4}\rangle_{nl} - s^2\left(\frac{1}{Q}\right)^2 \left(-2Q\langle r^{-2s-3}\rangle \right. \\ & \left. + l(l+1)\langle r^{-2s-4}\rangle + \frac{Q^2}{n^2}\langle r^{-2s-2}\rangle\right),\end{aligned} \tag{A3}$$

$$-\frac{Q^2}{n^2}\langle r^{-6}\rangle = -\frac{11Q}{5}\langle r^{-7}\rangle + \frac{3}{10}[(2l+1)^2 - 36]\langle r^{-8}\rangle. \tag{A4}$$

APPENDIX B

Expressions for α_d, α_Q, β_d, δ, and γ, including core fine-structure energies are given below. (Also Table III gives the matrix elements between *nLJ* states):

$$\alpha_d = \frac{1}{3}\sum_{n_c}\left(\frac{|\langle g\|\vec{D}\|n_c P_{1/2}\rangle|^2}{E(n_c P_{1/2})} + \frac{|\langle g\|\vec{D}\|n_c P_{3/2}\rangle|^2}{E(n_c P_{3/2})}\right), \tag{B1}$$

$$\alpha_Q = \frac{1}{5}\sum_{n_c}\left(\frac{|\langle g\|\vec{Q}\|n_c D_{3/2}\rangle|^2}{E(n_c D_{3/2})} + \frac{|\langle g\|\vec{Q}\|n_c D_{5/2}\rangle|^2}{E(n_c D_{5/2})}\right), \tag{B2}$$

$$\beta_d = \frac{1}{6}\sum_{n_c}\left(\frac{|\langle g\|\vec{D}\|n_c P_{1/2}\rangle|^2}{E(n_c P_{1/2})^2} + \frac{|\langle g\|\vec{D}\|n_c P_{3/2}\rangle|^2}{E(n_c P_{3/2})^2}\right), \tag{B3}$$

$$\gamma = \frac{1}{12}\sum_{n_c}\left(\frac{|\langle g\|\vec{D}\|n_c P_{1/2}\rangle|^2}{E(n_c P_{1/2})^3} + \frac{|\langle g\|\vec{D}\|n_c P_{3/2}\rangle|^2}{E(n_c P_{3/2})^3}\right), \tag{B4}$$

$$\begin{aligned}\delta = \frac{1}{30}\sum_{n_C, n_C'}\Bigg(&-2\sqrt{10}\frac{\langle g\|\vec{D}\|n_c P_{1/2}\rangle\langle n_c P_{1/2}\|\vec{D}\|n_c' D_{3/2}\rangle\langle n_c' D_{3/2}\|\vec{Q}\|g\rangle}{E(n_c P_{1/2})E(n_c' D_{3/2})} - 2\frac{\langle g\|\vec{D}\|n_c P_{3/2}\rangle\langle n_c P_{3/2}\|\vec{D}\|n_c' D_{3/2}\rangle\langle n_c' D_{3/2}\|\vec{Q}\|g\rangle}{E(n_c P_{3/2})E(n_c' D_{3/2})}\\ &+ 2\sqrt{6}\frac{\langle g\|\vec{D}\|n_c P_{3/2}\rangle\langle n_c P_{3/2}\|\vec{D}\|n_c' D_{5/2}\rangle\langle n_c' D_{5/2}\|\vec{Q}\|g\rangle}{E(n_c P_{3/2})E(n_c' D_{5/2})} + \sqrt{5}\frac{\langle g\|\vec{D}\|n_c P_{3/2}\rangle\langle n_c P_{3/2}\|\vec{Q}\|n_c' P_{3/2}\rangle\langle n_c' P_{3/2}\|\vec{D}\|g\rangle}{E(n_c P_{3/2})E(n_c' P_{3/2})}\\ &+ 2\sqrt{10}\frac{\langle g\|\vec{D}\|n_c P_{1/2}\rangle\langle n_c P_{1/2}\|\vec{Q}\|n_c' P_{3/2}\rangle\langle n_c' P_{3/2}\|\vec{D}\|g\rangle}{E(n_c P_{1/2})E(n_c' P_{3/2})}\Bigg).\end{aligned} \tag{B5}$$

[1] R. J. Drachman, Phys. Rev. A **26**, 1228 (1982).
[2] C. J. Kleinman, Y. Hahn, and L. Spruch, Phys. Rev. **165**, 53 (1968).
[3] K. Bockasten, Phys. Rev. A **9**, 1087 (1974).
[4] B. Edlen, in *Handbuch der Physik*, edited by S. Flugge, (Springer, Berlin, 1964), Vol. 27, pp. 125–129.
[5] R. A. Komara, M. A. Gearba, S. R. Lundeen, and C. W. Fehrenbach, Phys. Rev. A **67**, 062502 (2003).
[6] M. S. Safronova, W. R. Johnson, and A. Derevianko, Phys. Rev. A **60**, 4476 (1999).
[7] M. Safronova (private communication).
[8] L. J. Curtis, Phys. Rev. A **23**, 362 (1981).
[9] E. L. Snow, M. A. Gearba, R. A. Komara, S. R. Lundeen, and W. G. Sturrus, Phys. Rev. A **71**, 022510 (2005).
[10] NIST atomic spectra data base, http://physics.nist.gov/PhysRefData/ASD
[11] R. A. Komara, M. A. Gearba, C. W. Fehrenbach, and S. R. Lundeen, J. Phys. B **38**, S87 (2005).
[12] L. J. Curtis, Nucl. Instrum. Methods Phys. Res. **202**, 333 (1982).
[13] P. Vogel, Nucl. Instrum. Methods **110**, 241 (1973).
[14] C. J. Sansonetti, K. L. Andrew, and J. Verges, J. Opt. Soc. Am. **71**, 423 (1981).
[15] C. E. Theodosiou, Phys. Rev. A **28**, 3098 (1983).